JOURNAL OF CATALYSIS 10, 211–223 (1968)

Measurement of the State of Metal Dispersion on Supported Nickel Catalysts by Gas Chemisorption

C. S. BROOKS AND G. L. M. CHRISTOPHER

From the United Aircraft Research Laboratories, East Hartford, Connecticut 06108

Received July 31, 1967; revised December 19, 1967

Gas chemisorption has been investigated as a technique for the estimation of the state state of nickel dispersion on supported nickel hydrocarbon conversion catalysts. Published chemisorption studies on nickel catalysts are critically reviewed. Catalysts which were examined included nickel on alumina and nickel zeolites. Gas chemisorption measurements were supplemented by X-ray diffraction line-broadening determinations to establish the average nickel crystallite sizes.

Nickel areas estimated from hydrogen chemisorption at 250°C at a hydrogen vapor pressure of 100 mm mercury and from average nickel crystallite size determined by X-ray diffraction line-broadening were in good agreement. These results provide strong evidence that dissociative hydrogen adsorption occurs only on nickel crystallites of sufficient size to offer adjacent hydrogen adsorption sites. Carbon monoxide chemisorption at room temperature at a carbon monoxide vapor pressure of 100 mm mercury, after correction for carbon monoxide adsorption on the support, provides the more accurate measure of total nickel area including nickel in an atomic state of dispersion.

A combination of hydrogen chemisorption or X-ray diffraction line-broadening measurement, plus carbon monoxide chemisorption, can be used to estimate the relative amounts of nickel in comparatively large crystallites (~50 Å) and in an essentially atomic state of dispersion, as well as the specific surface area of the nickel in these two size ranges.

INTRODUCTION

The purpose of these experiments was to develop adequate chemisorption procedures for the estimation of the metal distribution on hydrocarbon conversion catalysts, specifically nickel on alumina and aluminosilicates (synthetic zeolites).

The gas–solid interfacial area available for gas–solid reactions is useful for a variety of reasons, such as a basis for reference of reaction kinetics to unit area, to evaluate catalyst development procedures where large specific surface areas are desired, and to understand the catalyst degradation processes such as poisoning and loss of reaction sites.

The total surface area is of primary importance for many catalysts, notably the various oxides. Supported metal catalysts, however, have distinctly different characteristics in that the principal reactive sites are considered to be on the surface of the metal phase which may be distributed in a discontinuous fashion partially covering the oxide support. Although nitrogen surface area measurements are adequate for the first class of catalysts, more specialized techniques are required to measure the metal surface areas of the second group—the supported metals.

The techniques fall into two principal categories: those which determine the effective metal particle-size distribution from which the metal surface area can be calculated and those which determine the metal surface area directly. The techniques of the first category include light microscopy, electron microscopy, and X-ray diffraction line-broadening. The principal technique in the second category is chemisorption of a gas which occurs with a high degree of

specificity on metal surfaces but not on oxide surfaces.

The chemisorption techniques have a very definite advantage over the particle-size techniques since the metal surface is measured directly by adsorption from the gas phase of an adsorbate molecule which in many instances closely resembles in size, shape, and chemical reactivity the molecules of interest in specific heterogeneous catalytic reactions. A limiting factor for the chemisorption technique is that a high order of specificity for adsorption of the selected adsorbate on the metal phase must be realized for accurate metal surface area determinations. Development of adequate chemisorption techniques requires that gas adsorption conditions be selected so that physical adsorption does not occur as a variable and indeterminate component in addition to the specific chemisorption on the metal phase. In addition, correction must be made for any adsorption component of the given gas on the oxide support. Also, che pretreatment and gas adsorption procedures must not significantly affect the state of metal distribution of the catalyst surface.

The feature of direct measurement of the gas–solid interfacial area afforded by the chemisorption techniques led to its selection for measurement of the available surface area of supported nickel metal catalysts on alumina and aluminosilicates. It is considered essential, however, to an adequate definition of the character of the metal structure of supported metal catalysts that chemisorption should be supplemented by a particle-size technique appropriate for the metal crystallite size distribution under study.

Among the most useful chemisorption phenomena applicable to supported metal catalysts are the activated adsorption of reactive gases, such as hydrogen and carbon monoxide on transition metals such as nickel, cobalt, platinum, etc. Chemisorption of hydrogen on transition metals has been investigated at temperatures from −196°C to 500°C. Chemisorption of carbon monoxide on the transition metals has been investigated from −196° to 75°C. The metals most extensively investigated have been iron (*1*, *2*, *3*), platinum (*4–16*), nickel (*17–25*), and to a lesser extent, cobalt (*26*, *27*) and palladium (*28*, *29*).

Published experiments on the chemisorption of hydrogen and carbon monoxide on nickel catalysts have demonstrated the dependence of the adsorption of these gases on temperature, pressure, character of the nickel preparation, and pretreatment history, The temperature dependence of either hydrogen or carbon monoxide adsorption on evaporated nickel films shows an approximately exponential character with a decline of about 20% between low temperature (−196° to −183°C) and room temperature (*2*, *3*). The temperature dependence for adsorption of both gases on the supported nickel catalysts is much greater than for the nickel films and changes of the order of factors of 2 or more occur. A reduced nickel oxide demonstrated the greatest heterogeneity with a greater hydrogen adsorption observed at 0°C than at −196°C and a minimum occurring around −175°C (*17*). In this last case the maximum observed at the higher temperature is attributed to an activated chemisorption which dominates when the temperature is raised from the low-temperature region where physical adsorption predominates.

The adsorption of both gases has an appreciable pressure dependence and nickel catalysts demonstrate changes by a factor of the order of 2 or more for changes in pressure from 10 mm of mercury to several hundred millimeters. This pressure dependence at any given temperature indicates that at least part of the adsorbed gas forms a relatively weak adsorption bond. Rideal and Trapnell (*20*) observed that a portion of the carbon monoxide adsorbed on nickel around room temperature has a heat of adsorption as low as 4 kcal/mole and of the magnitude to be expected for a purely physical adsorption process.

A disadvantage of most of the published experimental procedures for gas chemisorption at the lower part of the temperature range is that differentiation of chemisorption on the metal from physical adsorption on both the metal and the substrate becomes

a more difficult problem. A disadvantage at the upper part of the temperature range for both gases is that the probability increases for chemisorption on the substrate or other component, such as promoters present. The successful application of either hydrogen or carbon monoxide chemisorption to estimate metal surfaces requires selection of the conditions which will permit the most accurate corrections to be made for physical adsorption and chemisorption occurring on oxide substrates. In the present study the conditions which were selected as the most promising for development of a procedure were at the upper range of temperatures where physical adsorption would be at a minimum. The initial procedure development was with a nickel powder, to examine the effect of temperature on the adsorption of hydrogen and carbon monoxide on a nickel surface with no oxide support present. Evaluation was completed with nickel-alumina and nickel zeolite catalysts.

Experimental Procedures

Catalysts. The catalysts used in this study included several nickel-on-alumina catalysts (Girdler G56-1, G56-2, and G56-3) and several nickel zeolites prepared from Linde 13X, Norton Zeolon, and Davison Z14. The G56-2 and G56-3 differed from G56-1 in having smaller amounts of nickel and a lower surface area support. The nickel zeolites were prepared by ion exchange of the sodium exchange cations by nickel cations, followed by exhaustive water washing. The supported nickel catalysts were reduced 16 hr in a stream of 40 vol % high-purity hydrogen-helium mixture at 400°C to reduce the nickel cations to metallic nickel. The nickel powder used was a very fine particle size nickel obtained from the National Research Corporation, Cambridge, Massachusetts. The supported nickel catalysts were evacuated for 1 hr at 350°C to 10^{-5} torr and the nickel powder for 1 hr at 150°C to 10^{-5} torr in preparation for the gas adsorption measurements.

Gas preparation. The hydrogen and carbon monoxide gases used were of high purity, 99.95% and 99.5%, respectively, obtained from the Matheson Co., Inc., East Rutherford, New Jersey. These gases were further purified by passing over active platinum on asbestos at 300°C and over a molecular sieve adsorbent bed at liquid nitrogen temperature upon admission to the adsorption apparatus.

Chemical analyses. The nickel contents of the nickel-alumina and nickel zeolite catalysts were determined by standard wet procedures (dimethyl glyoxime precipitation). Chemical compositions of the zeolites are summarized in Table 1.

Apparatus. A conventional volumetric apparatus was used (*30*).

Carbon monoxide chemisorption. The carbon monoxide chemisorption procedure consisted of equilibration of a nickel catalyst (hydrogen-reduced) for 2 hr at a carbon

TABLE 1
Chemical Composition of Zeolites

Preparation designation	Zeolite	Principal cation		Minor cations (wt %)			CEC (meq/g)	
		Cation	Wt %	Na	Ca	Fe	Principal cation	Total cations
Na 13X	Linde 13X	Na^+	10.35[a]	—	0.81[a]	0.21[a]	4.49	5.01
Ni 13X	Linde 13X	Ni^{2+}	6.68[b]	5.20[a]	0.71[a]	0.26[a]	2.26	5.04
Na Zeolon	Norton Zeolon	Na^+	5.33[a]	—	0.76[a]	0.49[a]	2.32	2.96
Ni (Na) Zeolon	Norton Zeolon	Ni^{2+}	3.24[b]	2.23[a]	0.34[a]	0.57[a]	1.10	2.44
Na Dav Z14	Davison Z14	Na^+	6.71[a]	—	1.32[a]	0.46[a]	2.92	3.82
Ni Dav Z14	Davison Z14	Ni^{2+}	5.92[b]	2.19[a]	0.85[a]	0.35[a]	2.02	3.53

[a] Atomic absorption.
[b] Wet analysis.

monoxide vapor pressure of at least 400 mm Hg pressure at 23° ± 1°C, followed by measurement of a desorption isotherm down to a pressure of the order of 30 to 50 mm Hg pressure. The carbon monoxide adsorption on the catalyst support material alone was measured under the same conditions. The carbon monoxide adsorbate retained on the catalyst at 100 mm Hg pressure was used to estimate nickel distribution after correcting for any carbon monoxide adsorption on the support material at the same carbon monoxide vapor pressure.

Hydrogen chemisorption. The hydrogen chemisorption procedure consisted of equilibration of a nickel catalyst (hydrogen-reduced) for 2 hr at a hydrogen vapor pressure of about 600 mm Hg pressure at 250°C, then measuring several points on a desorption isotherm down to a vapor pressure of the order of 40 mm Hg pressure. This procedure is repeated a second and a third time with an evacuation at 10^{-5} torr for 1 hr at 350°C preceding each sequence of measurements. The irreversible hydrogen retention at 100 mm hydrogen vapor pressure is attributed to chemisorption on the nickel surface. Correction is made at the same temperature and hydrogen vapor pressure for the contribution of the support to the total hydrogen adsorption on the supported metal catalyst.

X-ray diffraction measurements. In addition to the gas adsorption measurements described above, average nickel crystallite sizes were determined by X-ray diffraction line-broadening procedures for a number of the nickel-on-alumina and nickel zeolite catalysts investigated in this study. These procedures have been described by Klug and Alexander (*31*). The samples were measured in a diffractometer unit using nickel-filtered copper radiation. The diffraction peaks were detected with a scintillation counter and pulse height analyzer and recorded on a strip chart. The natural instrumental line breadth of the diffractometer was measured with two materials, the (111) peak of coarse nickel powder and the (220) peak of sodium chloride. The line breadths from the two materials were found to be in close agreement and the data were used to calculate the average nickel crystallite sizes. X-ray diffraction powder patterns were determined for the nickel zeolites after ion exchange with nickel and water wash prior to hydrogen reduction and after hydrogen reduction at 400°C.

Results and Discussion

Catalyst Characterization

Chemical analyses established that the nickel content of the ion-exchanged zeolites used in the present studies represent 45% for Ni13X, 45% for Ni (Na) Zeolon, and 57% for nickel Davison Z14 of the total cation exchange capacities. The total cation exchange capacities were calculated from the sum of the sodium, calcium, nickel, and iron content of these zeolites (Table 1).

X-ray diffraction powder analyses of the nickel zeolites after ion exchange with nickel and water wash prior to hydrogen reduction at 400°C and after reduction in hydrogen at 400°C established that the zeolite lattice was crystallographically intact after ion exchange and after hydrogen reduction. This conclusion was based on examination of the interplanar *d* spacings and the relative intensities of the eight strongest lines selected from the powder pattern of the original sodium zeolite. The presence of nickel metal crystallites in the hydrogen-reduced Ni13X and Ni Dav Z14 zeolites was established by the presence of the five principal X-ray diffraction powder pattern lines of nickel. No detectable amount of nickel metal crystallites was found in the fresh hydrogen-reduced Ni (Na) Zeolon.

The effectiveness of the hydrogen reduction procedure at 400°C was established by reaction of nickel-alumina and nickel-zeolite catalysts with standard hydrochloric acid solutions and measurement of the amount of hydrogen evolution resulting from reaction with the metallic nickel present. A qualitative indication of metal reduction was observed in the darkening in color upon hydrogen reduction of both nickel-alumina and nickel-zeolite catalysts.

Temperature Dependence of Hydrogen and Carbon Monoxide Adsorption on Nickel Surfaces

The results of hydrogen and carbon monoxide adsorption measurements at several temperatures on a high-surface-area nickel metal powder and several zeolites are presented in Table 2. The results obtained on the nickel powder are quite similar to those obtained in previous published experiments on nickel catalysts. The ratio between carbon monoxide and hydrogen adsorption at 23°C and comparable vapor pressure finally attains a ratio of 1.2 after four successive hydrogen reductions and desorptions. The hydrogen adsorption capacity does not change significantly between room temperature and 150°C. The nickel zeolites demonstrated appreciable temperature dependence for adsorption of both gases in contrast to the nickel powder. The zeolite support, however, has a large adsorption capacity for carbon monoxide compared with hydrogen. Even after correction of the large carbon monoxide adsorption capacity of the zeolite support, the ratio of the carbon monoxide to the hydrogen adsorption at 23°C is three to six times the ratio observed on the nickel powder. The significance of this large difference between the adsorption of the two gases on the nickel zeolites is discussed in detail below the connection with the nickel crystallite size determinations by X-ray diffraction line-broadening.

It was concluded upon inspection of these results on the temperature dependence of the adsorption of both carbon monoxide and hydrogen that a temperature at the upper end of the scale would be most appropriate in view of the large adsorption capacity of the zeolite supports. Room temperature was selected as most suitable for carbon monoxide and 250° was chosen for hydrogen.

TABLE 2

ADSORPTION OF HYDROGEN AND CARBON MONOXIDE ON NICKEL POWDER AND NICKEL CATALYSTS

Adsorbent	Nickel content (wt %)	Gas	Pressure (mm Hg)	Adsorbate (cm^3/STP/g) −196°C	−78°C	25°C	150°C	250°C	Ratio CO/H_2 @ 25°C
Nickel		H_2	94.5	—	—	3.7	—	—	—
Powder		H_2	95	—	—	—	3.7	—	—
		CO	67	8.6	—	—	—	—	1.2
		CO	78	—	—	4.4	—	—	—
Na 13X		H_2	232	—	0.81	—	—	—	—
		H_2	127	—	—	0.37	—	—	—
		H_2	121	—	—	—	—	0.10	—
		CO	30.9	72.7	—	—	—	—	—
		CO	49.8	—	14.7	—	—	—	—
		CO	68.7	—	—	2.3	—	—	6.2
Ni 13XA-1	6.68	H_2	44.9	—	—	0.88	—	—	—
		CO	92.7	108.5	—	—	—	—	—
		CO	121.8	—	—	5.8	—	—	6.6
Ni Dav Z14	5.92	H_2	145	—		6.0	—	—	—
		H_2	42	—		—	—	0.76	—
		CO	90	147.6		—	—	—	3.4
		CO	57	—		20.8	—	—	—
Ni Zeolon	3.24	H_2	103.8	—		1.4	—	—	—
		H_2	39	—		—	—	0.10	—
		CO	61.8	61.9		—	—	—	4.3
		CO	167	—		6.1	—	—	—

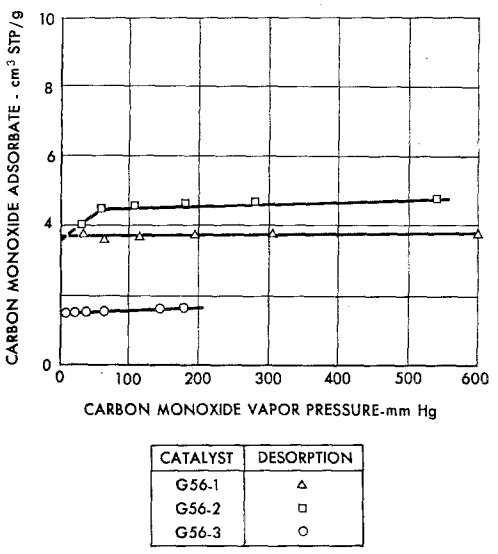

FIG. 1. Chemisorption of carbon monoxide on nickel-alumina catalysts at room temperature.

Carbon Monoxide Chemisorption

The results of the carbon monoxide chemisorption procedure on three nickel-on-alumina catalysts (Girdler G56-1, G56-2, and G56-3) are summarized in Fig. 1. The results for carbon monoxide chemisorption on two nickel zeolite catalysts (nickel Zeolon and nickel Davison Z14) are summarized in Table 3 and Figs. 2 and 3. The adsorption rate data for the nickel zeolites are shown in Figs. 2(a) and 3(a). It was found that at least 1 hr of equilibration was necessary for nickel on alumina and on the zeolites.

There was significant chemisorption of carbon monoxide at room temperature on the zeolite substrates so that all of the adsorption data for the nickel zeolites were

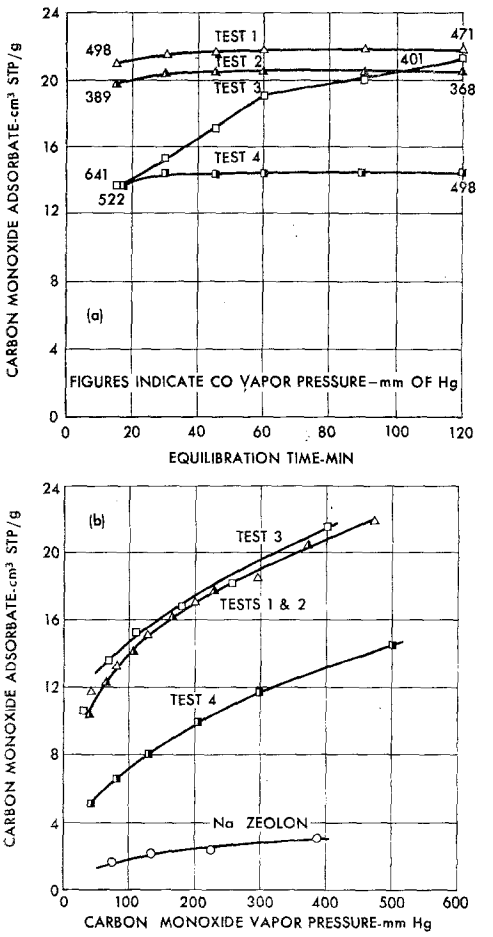

FIG. 2. Desorption of carbon monoxide at 23°C on nickel Zeolon.

TABLE 3

CHEMISORPTION OF CARBON MONOXIDE AT 23°C ON NICKEL ZEOLITES BY VOLUMETRIC PROCEDURES

Catalyst	Pretreatment	CO ads. at 100 mm Hg v.p. (cm³STP/g) Ni Zeol.	CO ads. at 100 mm Hg v.p. (cm³STP/g) Na Zeol.	CO chemisorbed on Ni (cm³STP/g)	Mole CO chemisorbed per Ni atom	Nickel content (wt %)	Test number Figs. 2, 3
Ni Zeolon	Unreduced; evac. 1 hr 350°C	14.0	1.9	12.1	0.98	3.24	1
Ni Zeolon	Unreduced; evac. 1 hr 350°C	14.0	1.9	12.1	0.98		2
Ni Zeolon	H_2 reduction 16 hr 400°C 20% H_2 in He; evac. 1 hr 350°C	14.7	1.9	12.8	1.03		3
Ni Zeolon	Same as above	7.3	1.9	5.4	0.44		4
Ni Dav Z14	Unreduced; evac. 1 hr 350°C	4.5	0.8	3.7	0.16	5.92	5
Ni Dav Z14	H_2 reduction 16 hr 400°C 20% H_2 in He; evac. 1 hr 350°C	7.6	0.8	6.8	0.31		6
Ni Dav Z14	Same as above	1.9	0.8	1.1	0.063		7

corrected by subtracting the carbon monoxide adsorbed on the sodium form of the zeolite from the total carbon monoxide adsorption on the nickel form to give the contribution due to the carbon monoxide chemisorption on nickel alone. Inasmuch as X-ray diffraction analyses established that ion exchange with nickel and hydrogen reduction have made no significant change in the crystallographic structure of the zeolite, it is considered safe to assume the adsorptive properties of the nickel zeolite substrate are essentially the same as the sodium zeolite. These data lead to the following conclusions:

(1) The observed ratio of one chemisorbed carbon monoxide molecule per nickel atom at 100 mm Hg vapor pressure demonstrates that the nickel is initially in an atomic state of dispersion in the case of nickel Zeolon.

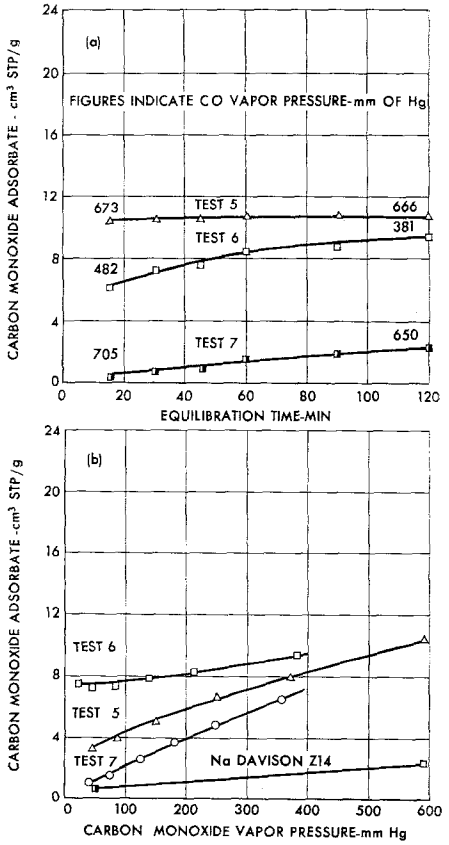

FIG. 3. Desorption of carbon monoxide at 23°C on nickel Davison zeolite Z14.

(2) In the case of both nickel Zeolon and nickel Davison zeolite, carbon monoxide chemisorption occurs just as quantitatively before hydrogen reduction as afterward. This means that carbon monoxide chemisorption can occur on nickel cations as well as on metallic nickel. This is discussed further below.

(3) The appreciable reduction in carbon monoxide adsorption capacity after the initial contact of both hydrogen-reduced zeolites with carbon monoxide indicates that heating the reduced nickel zeolite with carbon monoxide present as an adsorbate leads to surface migration and nickel crystallite growth, through formation and subsequent decomposition of nickel carbonyl. Confirmation of this effect was provided by X-ray diffraction line-broadening measurements of nickel crystallite size upon completion of the adsorption measurements.

(4) In the case of the nickel Davison zeolite the nickel distribution as indicated by X-ray diffraction measurements was substantially less than an atomic state of dispersion prior to carbon monoxide chemisorption.

Hydrogen Chemisorption

Hydrogen chemisorption was measured on five nickel catalysts which included three nickel-alumina Girdler catalysts (G56-1, G56-2, and G56-3) and two nickel zeolite catalysts (nickel Davison Z14 and nickel Norton Zeolon). The results of these experiments are summarized in Figs. 4 and 5. The conclusions warranted by these results include the following:

(1) The initial hydrogen uptake at 250°C which exceeded the subsequent hydrogen adsorption measurements for all the catalysts may be in part due to reduction of residual oxides on the nickel surface and in part to reaction with the zeolite substrate. Solubility of hydrogen in bulk-phase nickel at the maximum pressure used in these adsorption measurements could account for no more than ~0.002 cm³ STP/g for the highest nickel content catalyst used in these experiments (*32*).

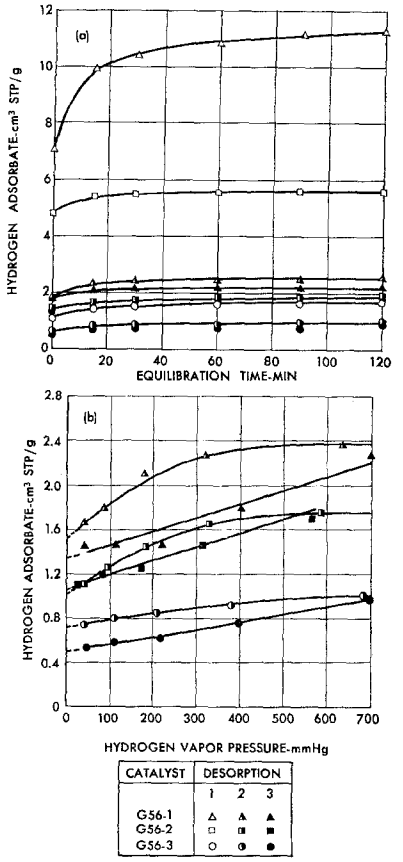

FIG. 4. Chemisorption of hydrogen on nickel-alumina catalysts at 250°C.

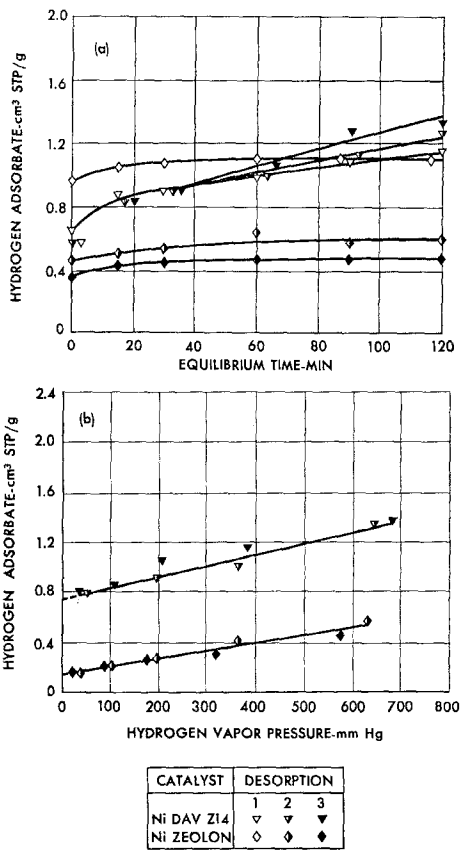

FIG. 5. Chemisorption of hydrogen on nickel zeolite catalysts at 250°C.

(2) The decrease in hydrogen adsorption between the second and third desorption indicates some sintering of the nickel occurred during the intervening evacuation at 350°C.

(3) The reproducibility is greater for the hydrogen chemisorption at 250°C than for the carbon monoxide chemisorption at 23°C. This is especially true for the nickel zeolites.

(4) The magnitude of the hydrogen chemisorption at 250°C is appreciably less than the carbon monoxide chemisorption at 23°C for all the catalysts. The significance of this fact is discussed in the next section.

(5) Hydrogen chemisorption at 250°C on the sodium forms of the Linde 13X, Davison Z14 zeolite, and Norton Zeolon yielded no adsorption values greater than the precision of the adsorption measurements (± 0.1 cm³ STP/g).

Comparison of Hydrogen and Carbon Monoxide Adsorption on Supported Nickel Catalysts

The negligible pressure dependence of the carbon monoxide adsorption on the nickel-alumina (Fig. 1) indicates that this adsorbate must be held in the main by irreversible chemisorption. The appreciable pressure dependence of carbon monoxide adsorption on nickel zeolites [Figs. 2(b), 3(b)] indicates that a large fraction of this adsorbate is held by reversible physical adsorption, presumably by the zeolite substrate. There was appreciable pressure dependence of the hydrogen adsorption on both nickel-alumina and nickel zeolites [Figs. 4(b), 5(b)]. This pressure dependence

amounted in some instances to as much as 50% of the total adsorption capacity between 400 and 50 mm of Hg vapor pressure. It seems improbable to assign this to a physical adsorption component at a temperature as elevated as 250°C, so that a weak chemisorption with low activation energy and heat of desorption could account for the observed performance with hydrogen.

Some of the results of the hydrogen and carbon monoxide adsorption on the nickel-alumina and nickel zeolite catalysts are summarized in Table 4. Comparison is made at two vapor pressures—400 and 50 mm Hg. Comparison is made at each vapor pressure for the hydrogen desorption isotherm at 250°C and the carbon monoxide desorption isotherm at 23°C. The mole ratio of the carbon monoxide to hydrogen adsorption at each vapor pressure on the nickel-alumina catalysts all lie within the range 1.6 to 3.6. This provides strong evidence that both gases see essentially the same adsorption sites, even considering the difference in temperature. The variations within a mole ratio range of 1.6 to 2.0 can be accounted for by having the major fraction of the carbon monoxide in linear (one carbon monoxide molecule per nickel atom) and a minor fraction in bridged (one carbon monoxide molecule per two nickel atoms) orientations. The situation for the nickel zeolites is quite different from the nickel-aluminas, mole ratios of 6.7 to 59 being obtained for carbon monoxide compared with hydrogen adsorption. Carbon monoxide apparently has access to many more adsorption sites than the hydrogen.

These gas chemisorption data can be used to estimate the nickel surface accessible for gas absorption by making certain assumptions. By employing the relationship,

$$\text{Surface nickel per g of catalyst} = Ni_S = \frac{2V(58.7)}{2.24 \times 10^4} \quad (1)$$

it is assumed that dissociative hydrogen adsorption occurs with one hydrogen atom for each surface nickel atom or molecular adsorption of carbon monoxide occurs with a bridged orientation between two nickel atoms. For the situation where one molecule of carbon monoxide adsorbs with a linear orientation on each surface nickel atom the factor 2 is omitted from the numerator in Eq. (1). Here V is the chemisorbed gas as cm³ at STP per gram and 2.24×10^4 is the molar volume in cm³ at STP of an ideal gas.

Eischens, Francis, and Pliskin (*33*) have assigned the two principal infrared absorption bands observed for carbon monoxide adsorbed on nickel to a linear

Ni—C═O

TABLE 4

A Comparison of Carbon Monoxide and Hydrogen Chemisorption on Supported Nickel Catalysts

Catalyst	Pressure (mm Hg)	Adsorbate (cm³STP/g) CO 23°C	Adsorbate (cm³STP/g) H_2 250°C	Mole ratio CO/H_2	Ni_s Surface Ni per g of catalyst H_2	Ni_s Surface Ni per g of catalyst CO linear	Ni_T Total Ni per g catalyst
G56-1	400	3.7	2.3	1.6	0.0121	0.0097	0.145
	50	3.6	1.7	2.1	0.00894	0.0094	
G56-2	400	4.7	1.7	2.8	0.00894	0.0123	0.131
	50	4.3	1.2	3.6	0.0063	0.0113	
G56-3	400	—	0.8	—	0.00422	—	0.0705
	100	1.5	0.6	2.5	0.00316	0.0039	
Ni Zeolon	400	18.4[a]	0.4	46	0.00211	0.0483	0.0324
	50	11.7[a]	0.2	59	0.00105	0.0307	
Ni Dav Z14	400	6.7[a]	1.0	6.7	0.00526	0.0185	0.0592
	50	6.7[a]	0.75	9.0	0.00395	0.0185	

[a] Corrected for CO adsorption on Na zeolite at same temperature and CO vapor pressure.

and to a bridged

carbon monoxide–nickel bonding. The bridged bond was considered the stronger of the two bonds. The linear bond demonstrated considerable pressure dependence, with the intensity of this absorption band increasing with increasing carbon monoxide vapor pressure. The linear carbon monoxide bonding provides the more reasonable basis for the treatment of the present adsorption data, as will be evident from the discussion below.

The relationship in Eq. (1) has considerable utility in that the amount of surface nickel, Ni_S, can be estimated without the limitations imposed by assuming effective molecular adsorbate coverage areas in order to estimate metal surface area (Table 4).

The surface nickel estimates for the nickel-alumina catalysts derived from the hydrogen (dissociative) and carbon monoxide (linear orientation) adsorption data agree within about 30%, with one exception, indicating that both gases are adsorbing on the same adsorption sites and further that the carbon monoxide must be predominantly in a linear orientation. Another significant conclusion is that the fraction of the total nickel in the surface for the nickel zeolites exceeds that of the nickel-alumina catalysts. The decline in metal area with repetition of the gas adsorption measurements is attributed primarily to the difficulty of degassing these nickel catalysts after exposure to either carbon monoxide or hydrogen without inducing nickel migration and crystallite growth during the degassing (Figs. 2–5). The initial carbon monoxide and hydrogen gas adsorption measurements after cleanup of residual surface nickel oxides are considered to be most representative of the original state of nickel dispersion on these catalysts. A further significant conclusion is that relatively low nickel loadings, e.g., around 3% in the case of the nickel Zeolon, are essential to maintain the initial atomic state of nickel dispersion.

Comparison of Nickel Metal Area Estimates from Gas Chemisorption and from X-Ray Diffraction Line-Broadening

Average nickel crystallite size estimates were made on the samples from the carbon monoxide chemisorption measurements at 23°C and from the hydrogen chemisorption measurements at 250°C using X-ray diffraction line-broadening. The results of these measurements are given in Tables 5 and 6. The data in these tables are treated in the following manner. The hydrogen and carbon monoxide chemisorption values obtained just prior to the X-ray diffraction measurements are first cited as cm^3 STP per gram and then expressed as nickel area in m^2 per gram. In the case of the carbon monoxide chemisorption on the zeolites, correction for the carbon monoxide chemisorption on the zeolite substrate has been made.

Total nickel metal area is given by the relation

$$\text{Nickel metal area as } m^2 \text{ per g catalyst} = S_T = \frac{VN\sigma}{(2.24 \times 10^4)(10^4)} \quad (2)$$

where N is Avogadro's number and σ is the effective molecular coverage area as cm^2 per adsorbate molecule. The values used for σ were 13×10^{-16} cm^2 per molecule for carbon monoxide (*23*) and 12×10^{-16} cm^2 per molecule for hydrogen (*3*). In the case of hydrogen it is considered that dissociative adsorption has occurred, yielding a value of 6×10^{-16} cm^2 per hydrogen atom. These molecular coverage areas approximate those for two-dimensional van der Waals constants or normal liquid packing density configurations. The quoted σ values from the literature were obtained principally from unsupported metal catalysts.

These gas chemisorption data can be used to estimate the amount of surface nickel employing Eq. (1). In the present calculations it was assumed that each surface nickel atom provided an adsorption

TABLE 5

NICKEL METAL AREA FROM CO CHEMISORPTION AT 23°C AND 100 MM HG CO VAPOR PRESSURE AND FROM X-RAY DIFFRACTION LINE-BROADENING

(1) Catalyst	(2) Total nickel content $\left(\frac{\text{g Ni}}{\text{g cat.}}\right)$ Ni_T	(3) CO chemisorbed $\left(\frac{\text{cm}^3\text{STP}}{\text{g}}\right)$	(4) Total nickel area $\left(\frac{\text{m}^2\text{Ni}}{\text{g cat.}}\right)$ S_T	(5) Surface nickel $\left(\frac{\text{g Ni}}{\text{g cat.}}\right)$ Ni_S	(6) Large particle size Ni $\left(\frac{\text{g Ni}}{\text{g cat.}}\right)$ (2) − (5) $Ni_T - Ni_S$	(7) X-Ray line broad., (Diam. Å)	(8) Nickel area large particle size $\left(\frac{\text{m}^2\text{Ni}}{\text{g Ni}}\right)$ S	(9) Nickel area large particle size $\left(\frac{\text{m}^2\text{Ni}}{\text{g cat.}}\right)$ (6) × (8) $S(Ni_T - Ni_S)$
G56-1	0.145	3.0	10	0.00787	0.1371	160	42.2	5.8
G56-2	0.131	3.8	13	0.00995	0.1211	125	53.9	6.5
G56-3	0.0705	1.5	5.2	0.0039	0.0666	365	18.5	1.2
Ni13XC	0.081	16.4	57	0.043	0.038	195	34.7	1.3
Ni13XB	0.15	5.8	20	0.0152	0.1348	310	21.8	2.9
NiDavZ14	0.0592	6.8	22	0.0197	0.0395	520	13.0	0.51
NiZeolon	0.0324	8.6	30	0.0225	0.0099	510	13.2	0.13
NiZeolon	0.0324	5.4	19	0.0141	0.0183	945	7.15	0.13

TABLE 6

NICKEL METAL AREA FROM HYDROGEN CHEMISORPTION AT 250°C AND 100 MM HG H_2 VAPOR PRESSURE AND FROM X-RAY DIFFRACTION LINE-BROADENING

(1) Catalyst	(2) Total nickel content $\left(\frac{\text{g Ni}}{\text{g cat.}}\right)$ Ni_T	(3) H_2 chemisorbed $\left(\frac{\text{cm}^3\text{STP}}{\text{g}}\right)$	(4) Total nickel area $\left(\frac{\text{m}^2\text{Ni}}{\text{g cat.}}\right)$ S_T	(5) Surface nickel $\left(\frac{\text{g Ni}}{\text{g cat.}}\right)$ Ni_S	(6) Large particle size Ni $\left(\frac{\text{g Ni}}{\text{g cat.}}\right)$ (2) − (5) $Ni_T - Ni_S$	(7) X-Ray line broad., (Diam. Å)	(8) Nickel area large particle size $\left(\frac{\text{m}^2\text{Ni}}{\text{g Ni}}\right)$ S	(9) Nickel area large particle size $\left(\frac{\text{m}^2\text{Ni}}{\text{g cat.}}\right)$ (6) × (8) $S(Ni_T - Ni_S)$
G56-1	0.145	1.5	4.8	0.00785	0.1372	155	43.5	6.0
G56-2	0.131	1.3	4.2	0.00680	0.1242	175	38.6	4.8
G56-3	0.0705	0.6	1.9	0.00314	0.0674	715	9.44	0.64
NiDavZ14	0.0592	0.85	2.7	0.00444	0.0548	185	36.6	2.0
NiZeolon	0.0324	0.20	0.65	0.00105	0.0314	680	9.9	0.31

site for a hydrogen atom or a carbon monoxide molecule.

The average crystallite size determinations by X-ray diffraction line-broadening were used to estimate the nickel metal specific surface area from the relation

$$\text{Nickel area in m}^2\text{ per g nickel} = S = \frac{6}{\rho\, d(10^4)} \quad (3)$$

where ρ is the nickel density and d is the crystallite diameter in cm, assuming spherical shape. The specific nickel surface area can be expressed also as nickel area per gram of catalyst from the relation

$$\text{Nickel area in m}^2\text{ per g catalyst} = S(Ni_T - Ni_S) \quad (4)$$

where Ni_T is the total nickel content per gram of catalyst from chemical analyses, Ni_S is the surface nickel content per gram of catalyst estimated from Eq. (1), and $(Ni_T - Ni_S)$ represents the nickel in large crystallites after correction for surface nickel.

The conclusions warranted by the data presented in Tables 5 and 6 are as follows:

(1) The nickel area estimates by hydrogen chemisorption agree well with the nickel area estimates from X-ray crystallite size for all five nickel catalysts, indicating that hydrogen chemisorption occurs primarily on the same nickel crystallites measured by X-ray diffraction line-broadening. This provides strong evidence that dissociative hydrogen adsorption occurs only on crystallites of sufficient size to afford adjacent hydrogen adsorption sites. An alternative explanation is that there is already appreciable labile hydrogen present on the surface

of the hydrogen-reduced nickel zeolite, even after degassing at 350°C and that this hydrogen forms some bond with the reduced surface nickel leading to an appreciable reduction in the amounts of hydrogen subsequently adsorbed at 250°C. Further work is required to resolve this point.

(2) Carbon monoxide chemisorption provides the only estimate of total surface nickel, including the contribution of nickel in an essentially atomic state of dispersion.

(3) A combination of hydrogen chemisorption or X-ray diffraction line-broadening plus carbon monoxide chemisorption can be used to estimate the relative amounts of nickel in an essentially atomic state of dispersion and in relatively large crystallites, as well as the specific surface area of the nickel in these two ranges of dispersion. A "large" crystallite is arbitrarily defined as $\geq$ 50 Å, which is the commonly accepted lower limit for metal average particle size estimates based on X-ray diffraction line-broadening measurements. The limits of precision for all of the X-ray particle size data presented here, however, indicate that "large" must be taken as 100 Å or greater.

The nickel zeolites show some very unique adsorptive behavior. Angell and Schaffer (*34*) have used infrared spectra to demonstrate that carbon monoxide forms adsorptive bonds with a number of divalent exchange cations on X and Y zeolites and Rabo, Angell, Kasai, and Schomaker (*35*) have used infrared, optical and ESR spectra to demonstrate that carbon monoxide forms adsorptive bonds with Ni^{2+} and Ni^{+} exchange cations on a Y zeolite. It is of special interest that on at least a portion of the cation exchange sites Ni^{2+} resists reduction to any lower valence state than Ni^{+} and that these latter adsorption sites can reversibly adsorb and desorb carbon monoxide and oxygen. In the experiments reported here it has been demonstrated that carbon monoxide can be reversibly adsorbed and desorbed on the unreduced nickel Zeolon and Davison Z14 (see tests 1, 2, 3, 5, and 6, Table 3) zeolites. Partial reduction of a portion of the Ni^{2+} exchange cations to Ni^{+} may lead to the persistence of nickel in an atomically disperse state and account for the sharp differentiation observed between the adsorptive behavior of these nickel zeolites toward carbon monoxide and hydrogen.

Acknowledgments

The authors express appreciation to Dr. G. Golden for the chemical analyses, to Mr. R. W. Anderson for the X-ray diffraction measurements, to Professor Paul H. Emmett for helpful discussions, and to the United Aircraft Corporation for permission to publish.

References

1. Emmett, P. H., and Brunauer, S., *J. Am. Chem. Soc.* **59**, 1553 (1937).
2. Beeck, O., Smith, A. E., and Wheeler, A. *Proc. Roy. Soc. (London)* **177A**, 62 (1940).
3. Beeck, O., *Advan. Catalysis* **2**, 151 (1950).
4. Spenadel, L., and Boudart, M., *J. Phys. Chem.* **64**, 204 (1960).
5. Adler, S. F., and Kearney, J. J., *J. Phys. Chem.* **64**, 208 (1960).
6. Herrmann, R. A., Adler, S. F., Goldstein, M. S., and deBaur, R. M., *J. Phys. Chem.* **65**, 2189 (1961).
7. Hughes, T. R., Houston, R. J., and Sieg, R. P., *Ind. & Eng. Chem. Process Design Develop.* **1**, 96 (1962).
8. Adams, C. R., Benesi, H. A., Curtis, R. M., and Meisenheimer, R. G., *J. Catalysis* **1**, 336 (1962).
9. Gruber, H. L., *Anal. Chem.* **13**, 1828 (1962).
10. Gruber, H. L., *J. Phys. Chem.* **66**, 48 (1962).
11. Hall, W. K., and Lutinski, F. E., *J. Catalysis* **2**, 518 (1963).
12. Maat, H. J., and Moscou, L., *Proc. Intern. Congr. Catalysis, 3rd, Amsterdam, 1964* **2**, 1277. (North Holland Publ. Co., and Wiley, 1965).
13. Poltorak, O. M., and Boronin, V. S., *Russ. J. Phys. Chem. (Engl. Transl.)* **39**, 781–785 (1965).
14. Benson, J. E., and Boudart, M., *J. Catalysis* **4**, 704 (1965).
15. Boudart, M., Aldag, A. A., Benson, J. E., Dougharty, N. A., and Harkins, C. G., *J. Catalysis* **6**, 92 (1966).
16. Hightower, J. W., and Emmett, P. H., *J. Colloid Interface Sci.* **22**, 158 (1966).
17. Benton, A. F., and White, T. A., *J. Am. Chem. Soc.* **52**, 2325 (1930).
18. Emmett, P. H., and Skau, N., *J. Am. Chem. Soc.* **65**, 1029 (1943).
19. Sadek, H., and Taylor, H. S., *J. Am. Chem. Soc.* **72**, 1168 (1950).

20. RIDEAL, E. K., AND TRAPNELL, B. M. W., *Proc. Roy. Soc.* (*London*) **A205**, 409 (1951).
21. BAKER, M. McD., JENKINS, G. I., AND RIDEAL, E. K., *Trans. Faraday Soc.* **51**, 1592 (1955).
22. SCHUIT, G. C. A., AND VAN REIJEN, L. L., *Advan. Catalysis* **10**, 242 (1958).
23. KOKES, R. J., AND EMMETT, P. H., *J. Am. Chem. Soc.* **82**, 1037 (1960).
24. VLASENKO, V. M., KUKHAR, L. A., RUSOV, M. T., AND SAMCHENKO, N. P., *Kinetics Catalysis* (*USSR*) (*Engl. Transl.*) **5**, 301–337 (1964).
25. CARTER, J. L., AND SINFELT, J. H., *J. Phys. Chem.* **70**, 3003 (1966).
26. ANDERSON, R. B., HALL, W. K., AND HOFER, H. J. E., *J. Am. Chem. Soc.* **70**, 2465 (1948).
27. SASTRI, M. V. C., VISWANATHAN, T. S., AND NAGARJUNAN, T. S., *J. Phys. Chem.* **63**, 518 (1959).
28. SCHOLTEN, J. J. F., AND VAN MONTFOORT, A., *J. Catalysis* **1**, 85 (1962).
29. KAWASAKI, K., SUGITA, T., AND EBISAWA, S., *J. Chem. Phys.* **44**, 2313 (1966).
30. FAETH, P. A., Rept. No. 66110-2-X, Inst. Sci. Technol., Univ. Michigan, Ann Arbor, October, 1962.
31. KLUG, H. P., AND ALEXANDER, L. E., "X-Ray Diffraction Procedures," Chap. 9. Wiley, New York, 1954.
32. DUSHMAN, S., "Scientific Foundations of Vacuum Technique," pp. 559–560. Wiley, New York, 1949.
33. EISCHENS, R. P., FRANCIS, S. A., AND PLISKIN, W. A., *J. Phys. Chem.* **60**, 194 (1956).
34. ANGELL, C. L., AND SCHAFFER, P. C., *J. Phys. Chem.* **70**, 1413 (1966).
35. RABO, J. A., ANGELL, C. L., KASAI, P. H., AND SCHOMAKER, V., *Discussions Faraday Soc.* **41**, 328 (1966).